Kikuchi *et al. Respiratory Research* (2024) 25:330
https://doi.org/10.1186/s12931-024-02958-0

Respiratory Research

RESEARCH Open Access

Recombinant thrombomodulin and recombinant antithrombin attenuate pulmonary endothelial glycocalyx degradation and neutrophil extracellular trap formation in ventilator-induced lung injury in the context of endotoxemia

Kenichiro Kikuchi[1], Satoshi Kazuma[2*] and Michiaki Yamakage[1]

Abstract

Background Vascular endothelial damage is involved in the development and exacerbation of ventilator-induced lung injury (VILI). Pulmonary endothelial glycocalyx and neutrophil extracellular traps (NETs) are endothelial protective and damaging factors, respectively; however, their dynamics in VILI and the effects of recombinant thrombomodulin and antithrombin on these dynamics remain unclear. We hypothesized that glycocalyx degradation and NETs are induced by VILI and suppressed by recombinant thrombomodulin, recombinant antithrombin, or their combination.

Methods VILI was induced in male C57BL/6J mice by intraperitoneal lipopolysaccharide injection (20 mg/kg) and high tidal volume ventilation (20 mL/kg). In the intervention groups, recombinant thrombomodulin, recombinant antithrombin, or their combination was administered at the start of mechanical ventilation. Glycocalyx degradation was quantified by measuring serum syndecan-1, fluorescence-labeled lectin intensity, and glycocalyx-occupied area in the pulmonary vascular lumen. Double-stranded DNA in the bronchoalveolar fluid and fluorescent areas of citrullinated histone H3 and myeloperoxidase were quantified as NET formation.

Results Serum syndecan-1 increased, and lectin fluorescence intensity decreased in VILI. Electron microscopy revealed decreases in glycocalyx-occupied areas within pulmonary microvessels in VILI. Double-stranded DNA levels in the bronchoalveolar lavage fluid and the fluorescent area of citrullinated histone H3 and myeloperoxidase in lung tissues increased in VILI. Recombinant thrombomodulin, recombinant antithrombin, and their combination reduced glycocalyx injury and NET marker levels. There was little difference in glycocalyx injury and NET makers between the intervention groups.

*Correspondence:
Satoshi Kazuma
sea_hawk_3104@yahoo.co.jp

Full list of author information is available at the end of the article

Conclusion VILI induced glycocalyx degradation and NET formation. Recombinant thrombomodulin and recombinant antithrombin attenuated glycocalyx degradation and NETs in our VILI model. The effect of their combination did not differ from that of either drug alone. Recombinant thrombomodulin and antithrombin have the potential to be therapeutic agents for biotrauma in VILI.

Keywords Biotrauma, Glycocalyx, Neutrophil extracellular traps, Recombinant antithrombin, Recombinant thrombomodulin, Ventilator-induced lung injury

Background

Mechanical ventilation can cause ventilator-induced lung injury (VILI) [1] in patients with acute respiratory distress syndrome (ARDS). Mechanical stress on alveoli and inflammatory mediators released by activated neutrophils impair vascular endothelial function [2]. Impaired pulmonary vascular endothelial integrity mediates the pathogenesis and exacerbation of lung injury and causes remote-organ damage (biotrauma) [3].

The elucidation of the mechanisms of pulmonary vascular endothelial cell injury could help to clarify VILI pathogenesis. However, few reports have described the role of the endothelial glycocalyx (eGCX) in VILI. eGCX, present on vascular endothelial cells, regulates vascular permeability, anticoagulation, and leukocyte adhesion [4]. Neutrophil extracellular traps (NETs), released by activated neutrophils, have been implicated in VILI [5]. Clinical and in vivo studies have reported that NETs induce eGCX shedding from the vascular endothelium, and NETs have been implicated in the loss of normal vascular endothelial function through exposure and activation of endothelial cells [6–8]. eGCX and NETs could be therapeutic targets for alleviating biotrauma in VILI.

Recombinant thrombomodulin (rTM) and recombinant antithrombin (rAT) are used in clinical practice for the treatment of disseminated intravascular coagulation and have been reported as potential therapeutic agents for eGCX- and NET-targeted treatment [9–12]. rTM mitigates eGCX injury through its anti-inflammatory effects and upregulates eGCX synthesis [9]. rAT inhibits NET release through histone degradation, suppresses neutrophil activation and migration [13, 14], and diminishes eGCX injury through its anti-inflammatory effects and vascular endothelial repair capability [10]. rAT inhibits NET release by suppressing neutrophil activation [15] and accelerates NET clearance by directly binding to NETs [16].

The use of rTM, rAT, or their combination for VILI, targeting eGCX and NET kinetics, has not been reported. In this study, we focused on the dynamics of eGCX and NETs in VILI, with rTM, rAT, or their combination as interventions. We hypothesized that high tidal volume ventilation (HTV) with lipopolysaccharide would induce VILI, eGCX degradation, and NET formation. We also hypothesized that prophylactic administration of rTM, rAT, or their combination would alleviate lung injury, eGCX degradation, and NET formation in VILI.

Methods

Animals

All experiments were performed on 8–12-week-old male C57BL/6J mice. Mice were maintained on a 12-h light/12-h dark cycle with free access to food and water in a temperature- and humidity-controlled environment (at 23 °C ± 3 °C and 55% ± 20%).

Experimental groups

The mice were randomized into seven experimental groups (N=6/group; Fig. 1): the control group included mice breathing spontaneously for 4 h; the lipopolysaccharide (LPS) group included mice receiving an intraperitoneal injection of LPS (20 mg/kg) derived from *Escherichia coli* O55:B5 (Sigma-Aldrich, St. Louis, MO, USA) and breathing spontaneously for 4 h; the mice in the remaining groups received an intraperitoneal injection of 20 mg/kg LPS and were mechanically ventilated for 4 h, i.e., the low tidal volume ventilation (LTV) and high tidal volume ventilation (HTV) groups were subjected to low (tidal volume: 6 mL/kg, respiratory rate: 140/min) and high (tidal volume: 20 mL/kg; respiratory rate: 70/min) tidal volume ventilation, respectively. The LTV group was established to evaluate the possible effect of mechanical ventilation on lung injury, inflammation, glycocalyx, and NETs. The rTM, rAT, and rTMAT groups received HTV and intraperitoneal injections of 30 mg/kg rTM, 750 IU/kg rAT, and both, respectively. LPS was diluted in a total volume of 100 μL phosphate-buffered saline (PBS); rTM and rTA were diluted in a total volume of 100 μL saline. The control group received the same volume of PBS as the LPS group. The LPS, LTV, and HTV groups received the same volumes of saline instead of rTM and rAT. The rTM group received the same volume of saline. The rAT group received an equal volume of saline instead of rTM.

Experimental protocol

After mice were anesthetized with an intraperitoneal injection containing 0.3 mg/kg medetomidine hydrochloride (Nippon Zenyaku Kogyo Co., Ltd., Fukushima, Japan), 4 mg/kg midazolam (Astellas Pharma Inc., Tokyo, Japan), and 5 mg/kg butorphanol tartrate (Meiji Seika

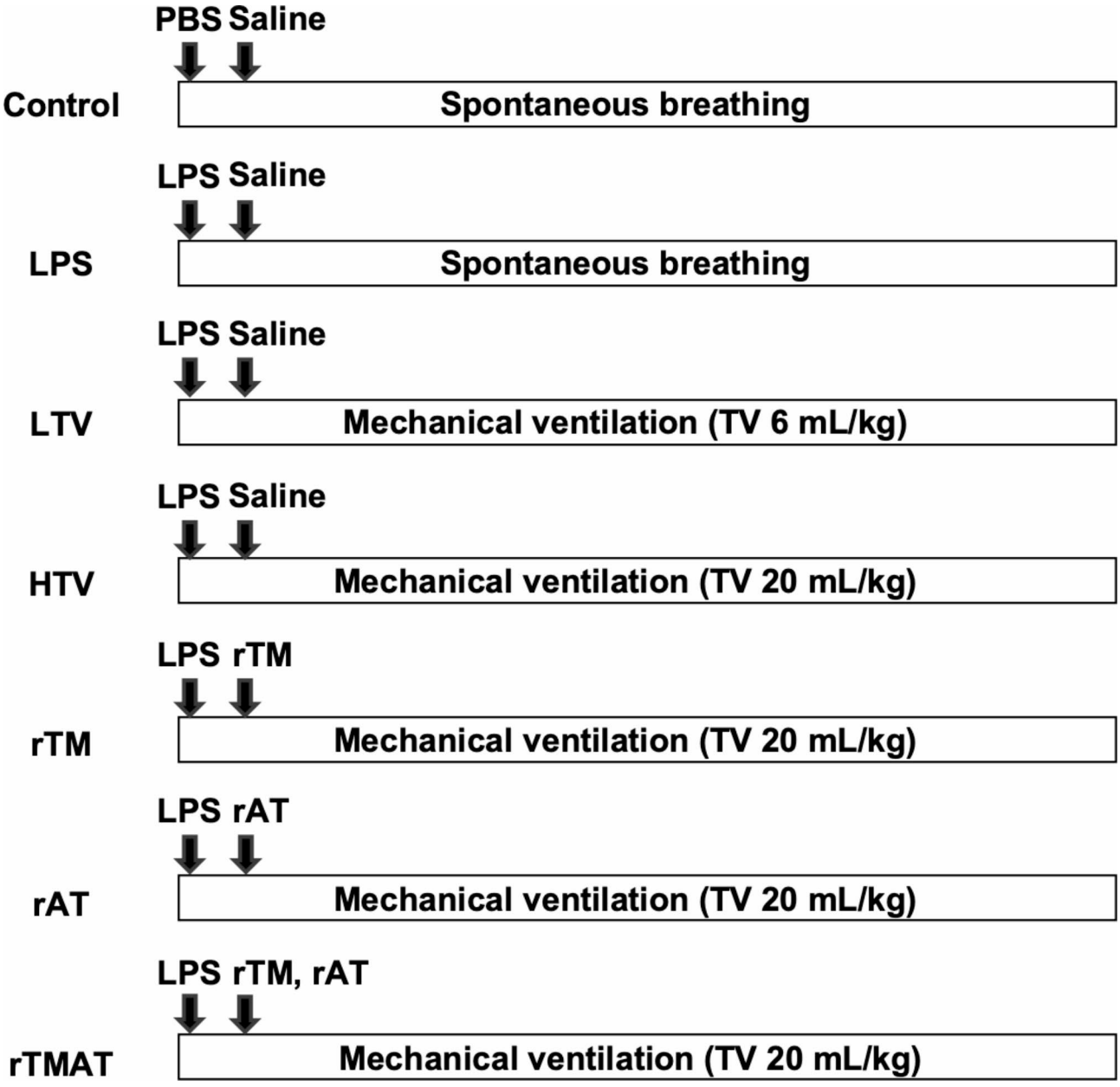

Fig. 1 Experimental timeline for each group. The control and LPS groups breathed spontaneously, whereas the other groups were mechanically ventilated for 4 h. The LTV group was mechanically ventilated with a tidal volume of 6 mL/kg and a respiratory rate of 140/min. The HTV, rTM, rAT, and rTMAT groups were mechanically ventilated with tidal volume of 20 mL/kg and respiratory rate of 70/min. LPS (20 mg/kg) was administered immediately after the initiation of mechanical ventilation. rTM and/or rAT were administered immediately after LPS injection. PBS = phosphate-buffered saline; TV = tidal volume; LPS = lipopolysaccharide; rTM = recombinant thrombomodulin; rAT = recombinant antithrombin; LTV = low tidal volume ventilation; HTV = high tidal volume ventilation

Pharma Co. Ltd., Tokyo, Japan) [17], tracheostomies were performed. Mechanical ventilation using the R415 VentStar Small Animal Ventilator (RWD Life Science Co., Shenzhen, China) was started immediately after a 20-gauge plastic cannula (TERUMO, Tokyo, Japan) was inserted into the trachea. The trachea was ligated using a 4−0 nylon thread to prevent gas leakage. Muscle relaxation was achieved by intraperitoneal rocuronium injection (4 mg/kg; MSD Co., Tokyo, Japan), and subcutaneously administered acetate Ringer's solution (0.5 mL) was used as the resuscitation fluid. Mechanical ventilation was maintained for 4 h using a inspiratory oxygen fraction of 0.3 in a volume-controlled mode in HTV and LTV; the ventilator was set to a tidal volume of 20 mL/kg body weight, frequency 70/min, and positive end-expiratory pressure 0 cm H_2O and 6 mL/kg, frequency

140/min, and positive end-expiratory pressure 0 cm H_2O, respectively. PEEP was set to 0 to exclude the effect of PEEP differences on the lungs and to investigate the effect of tidal volume on VILI. The respiratory rate was set to avoid excessive hyper- or hypocapnia in both low tidal ventilation and high tidal ventilation. Our preliminary study showed that after 4-h mechanical ventilation, respiratory rate settings resulted in partial pressures of carbon dioxide of 40–50 mmHg. An alveolar recruitment maneuver (5-s of inspiratory pressure held at 30 cmH_2O) was performed every 60 min. The temperature of all mice was maintained at 36.5 °C±0.5 °C using a thermal blanket (BWT-100 A; Bio Research Center Co. Ltd., Nagoya, Japan). At the end of the protocol, blood samples were collected from the left ventricle, and bronchoalveolar lavage fluid (BALF) was obtained from the left lung. Whole blood was allowed to clot for 2 h at room temperature of 22℃–25℃ and then centrifuged at 2,000 × *g* for 20 min at 4℃. The supernatant was collected and stored at −80℃ for further experiments. BALF was centrifuged at 500 × *g* for 5 min at 4℃ and stored at −80℃ until analysis. After the mice were killed, their lungs were extracted. No mice died during the 4 h of our experimental protocol in either group.

Systemic and pulmonary inflammation

Serum TNF-α and HMGB-1 levels were measured to assess systemic inflammation, whereas TNF-α and HMGB-1 levels in BALF, the number of inflammatory cells in BALF, and the percentage of neutrophils in BALF were measured to assess pulmonary inflammation. TNF-α (MTA00B; R&D Systems, Minneapolis, MN, USA) and HMGB-1 (Shino-test, Tokyo, Japan) [18] levels in serum and BALF were measured using enzyme-linked immunosorbent assay (ELISA) kits. After centrifugation, cell pellets were resuspended in 0.5 mL PBS, and the total number of cells in the BALF was measured using a cell counter. Cytocentrifuge slides of BALF cells were fixed in methanol and stained with Diff-Quick (Sysmex Co., Hyogo, Japan). Neutrophil percentage in BALF was calculated as the percentage of neutrophils within approximately 300 granulocytes [19].

Pulmonary vascular permeability

Pulmonary vascular permeability was assessed using the wet-to-dry ratio of the lung and albumin levels in the BALF. Harvested lungs were weighed, and then each sample was desiccated in a warm cabinet at 65 °C for 24 h and reweighed. The wet-to-dry ratio of each sample was calculated. BALF albumin levels were measured using ELISA kits (E99-134; Bethyl Laboratories, Inc., Waltham, MA, USA) [20].

Lung histology

The left lung tissue was fixed in 10% formalin and embedded in paraffin. Thereafter, 3-μm-thick paraffin sections were deparaffinized and rehydrated. Finally, the slides were counterstained with hematoxylin and eosin. The VILI score, a lung injury scoring system, was used to assess the degree of lung injury, as previously described with some modifications [21]. Five random representative images were selected from each lung (400× magnification). In each representative image, 10 alveolar walls were randomly selected to measure thickness. The number of inflammatory cells and degree of hemorrhage were measured in each image. Alveolar wall thickness, inflammatory cell infiltration, and hemorrhage were graded according to a five-point scale: 0, minimal damage; 1, mild damage; 2, moderate damage; 3, severe damage; and 4, maximal damage. The degree of lung injury was quantitatively assessed by adding up scores, ranging from 0 to 12, for each image. The average score for each image was compared between groups. All images of the hematoxylin and eosin-stained sections were captured using an all-in-one fluorescence microscope (BZ-X710; KEYENCE, Osaka, Japan). The VILI scores were scored in a blinded fashion.

Lung mechanics

Lung mechanics were assessed for each group by intra- and intergroup comparisons of peak inspiratory pressure (PIP) and dynamic lung compliance (DLP). PIP displayed on the ventilator was recorded at the start of mechanical ventilation; at 1 h, 2 h, and 3 h after the initiation of ventilation; and at the end of mechanical ventilation. PIP was recorded immediately after alveolar recruitment maneuver at the start of mechanical ventilation and just before alveolar recruitment maneuver at 1, 2, 3, and 4 h. DLP was calculated as the ratio of the tidal volume to PIP (tidal volume/PIP).

Glycocalyx degradation

Glycocalyx degradation was assessed using serum syndecan-1 levels, lung immunofluorescence staining with lectin, and the occupied area of the glycocalyx of microvessels was examined using transmission electron microscopy (TEM). Serum syndecan-1 levels were measured using ELISA quantitation kits (860.090.192; Diaclone SAS, Besancon, France) [22]. A portion of the excised right lung was embedded in the OCT compound (Sakura Finetek, Tokyo, Japan) and frozen at −80℃. Next, 8-μm-thick frozen lung sections were prepared with a cryostat and incubated at room temperature for 1 h with DyLight594 Lycopersicon esculentum lectin (1:100, DL-1177; Vector Laboratories, Burlingame, CA, USA). Vector TrueVIEW (SP-8500, Vector Laboratories) was used to remove unwanted autofluorescence in

accordance with the manufacturer's protocol. Lectin fluorescence intensity was manually scored in 10 high-power fields per sample using a fluorescence microscope and ImageJ ver. 2.3.0 (National Institutes of Health, Bethesda, MD, USA), as described previously [10].

Electron microscopy

After 4 h of the experimental protocol, the mice were deeply anesthetized and perfused through a cannula placed in the left ventricle at a steady rate of 1 mL/min with a solution comprising 2% glutaraldehyde, 2% sucrose, 0.1 M sodium cacodylate buffer, and 2% lanthanum nitrate via a perfusion pump (TERUMO, Tokyo, Japan). The lungs were harvested, and lung tissues were processed for TEM, as previously reported [23]. The eGCX occupation area on capillary lumens was measured in six randomly selected capillary vessels in TEM images [24]. Lectin fluorescence intensity and glycocalyx-occupied areas were scored in a blinded fashion.

Lung NET formation

Lung NETs were quantified using BALF double-stranded DNA (ds-DNA) levels and the percentage of citrullinated histone H3 and myeloperoxidase (MPO) fluorescence area in immunofluorescence. BALF ds-DNA levels were measured using a NanoDrop One spectrophotometer (13-400-518; Thermo Fisher Scientific, Waltham, MA, USA). Harvested lungs were embedded in OCT compound, frozen at −80℃, and cryosectioned at 8 μm. The sections were fixed with cold acetone for 15 min and blocked with 3% bovine serum albumin in PBS for 1 h at a room temperature of 22℃–25℃. Lung sections were incubated overnight at 4℃ with rabbit anti-mouse citrullinated histone H3 antibody (1:500, ab5103, Abcam, Cambridge, UK) and goat anti-mouse MPO antibody (1:100, AF3667, R&D Systems) as the primary antibodies. After washing, sections were incubated with Alexa 488-donkey anti-rabbit IgG (1:500, ab150073; Abcam) and Alexa 594-donkey anti-goat IgG (1:500, ab150132; Abcam) for 1 h at room temperature. DNA was stained with VECTASHIELD Vibrance Antifade Mounting Medium (H-1800; Vector Laboratories). Images were captured using an all-in-one fluorescence microscope (BZ-X710). From the respective lung sections, each comprising an area of approximately 1.6 mm^2, the percentages of citrullinated histone H3-positive and MPO-positive areas in each field were calculated in two randomly selected non-overlapping fields. The percentage of positive areas was averaged for each organ and individual animal. Image analysis was performed using ImageJ. NETs areas were scored in a blinded fashion.

Statistical analyses

Sample sizes were calculated using G*power 3.1 (Heinrich-Heine-University, Düsseldorf, Germany) to detect differences in serum syndecan-1 levels. The sample size calculation was based on a comparison between VILI and rTM. In our pilot study, we compared the serum syndecan-1 levels between VILI (n=4) and rTM mice (n=4). The serum syndecan-1 levels in the HTV and rTM groups were 5.8±2.2 (mean±standard deviation) and 2.6±0.5 ng/mL, respectively. The effect size was calculated to be 2.0. A sample size of 6 mice per group was considered adequate based on our pilot study results (α=0.05, 1−β=0.8, two-tailed, sample size ratio=1). All data were tested for normal distribution using the Shapiro–Wilk test. One-way ANOVA was used to compare groups, followed by the Tukey post-hoc test. PIP and DLP at different time points were analyzed using two-way ANOVA for repeated measures. Quantitative data are presented as mean±standard error of the mean. All calculations were performed using Prism 9 (GraphPad, La Jolla, CA, USA). Statistical differences were considered significant at P<0.05.

Results

Effect of rTM and/or rAT on systemic inflammation in VILI

We investigated whether LPS administration and HTV for 4 h induced systemic inflammation. Serum TNF-α levels at 4 h after LPS administration increased approximately 130-fold (P=0.90) and were even approximately 9-fold higher in the HTV group than in the LPS group (P<0.0001). rTM, rAT, and rTMAT decreased serum TNF-α levels by half (P<0.0001, P=0.0002, and P=0.0007, respectively; Fig. 2A). Serum HMGB-1 levels did not increase after 4 h of LPS administration but increased 4-fold with LPS and HTV (P>0.99 and P<0.0001, respectively). rTM, rAT, and rTMAT reduced serum HMGB-1 levels (P<0.0001, P=0.0013, and P=0.024, respectively; Fig. 2B).

Effect of rTM and/or rAT on pulmonary inflammation in VILI

BALF TNF-α levels increased approximately 150-fold in the HTV group compared with those in the control group (P<0.0001). rTM, rAT, and rTMAT reduced BALF TNF-α levels by half, and a significant reduction was seen in only the rTMAT group (P=0.07, P=0.06, and P=0.019, respectively; Fig. 2C). Compared with the control group, BALF HMGB-1 levels increased approximately 7-fold in the HTV group (P=0.0001). BALF HMGB-1 levels were reduced in the rTM, rAT, and rTMAT groups (P=0.013, P=0.0017, and P=0.0031, respectively; Fig. 2D). The number of inflammatory cells in BALF was 3.9-fold higher in the HTV group than in the control group (P<0.0001). The number of inflammatory cells decreased in the rTM, rAT, and rTMAT groups compared with that

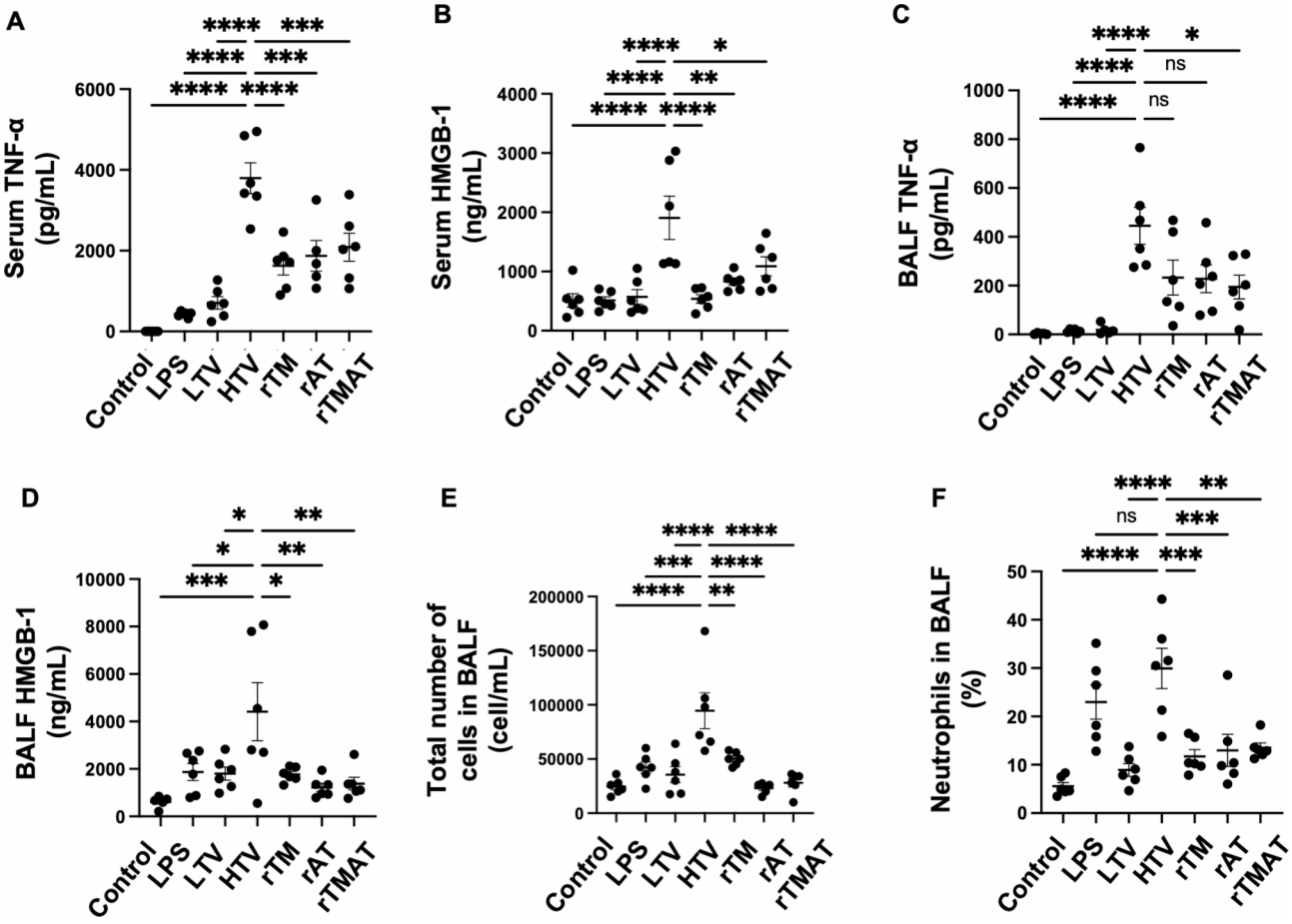

Fig. 2 Systemic and pulmonary inflammation. **A** and **B**) Serum TNF-α ($N=5$–6) and HMGB-1 levels ($N=6$) after 4 h of mechanical ventilation or spontaneous breathing. **C**) BALF TNF-α levels ($N=5$–6). **D**) BALF HMGB-1 levels ($N=6$). **E**) Total inflammatory cell counts in BALF ($N=6$). **F**) The percentage of neutrophils in BALF ($N=6$). ns = not significant. *$P \le 0.05$, **$P \le 0.01$, ***$P \le 0.001$, ****$P \le 0.0001$. BALF = bronchoalveolar lavage fluid

in the HTV group ($P=0.0029$, $P<0.0001$, and $P<0.0001$, respectively; Fig. 2E). The percentage of neutrophils was 5.5% ± 0.78%, 23.0% ± 3.6%, and 29.9% ± 4.2% in the control, LPS, and HTV groups, respectively ($P=0.0006$, control vs. LPS group; $P<0.0001$, control vs. HTV group). The percentage of neutrophils significantly decreased following rTM, rAT, and rTMAT administration ($P=0.0003$, $P=0.0008$, and $P=0.0013$, respectively; Fig. 2F). No significant difference in the degree of systemic or pulmonary inflammation was observed between the treatment groups.

Effect of rTM and/or rAT on pulmonary vascular permeability in VILI

Vascular hyperpermeability in the lungs increases pulmonary water content and BALF albumin levels. Elevated wet-to-dry ratio and BALF albumin levels represent pulmonary vascular hyperpermeability. The wet-to-dry ratio was higher in the HTV group than in the control and LPS groups ($P<0.0001$ and $P=0.0001$, respectively). rTM, rAT, and rTMAT significantly decreased the wet-to-dry ratio ($P=0.0052$, $P=0.0006$, and $P=0.0052$, respectively; Fig. 3A). BALF albumin levels were higher in the HTV group than in the control, LPS, and LTV groups ($P=0.0003$, $P=0.0001$, and $P=0.0008$, respectively). BALF albumin levels were significantly reduced in the rTMAT groups compared with those in the HTV group ($P=0.032$; Fig. 3B).

Effect of rTM and/or rAT on lung histology in VILI

Alveolar wall thickening, neutrophil infiltration, and hemorrhage were observed in the HTV group compared with those in the control, LPS, and LTV groups (Fig. 4A–D). The rTM, rAT, and rTMAT groups showed less alveolar wall thickening, neutrophil infiltration, and hemorrhage compared with the HTV group (Fig. 4E–G). The VILI scores of the HTV group were significantly higher than those of the control, LPS, and LTV groups ($P<0.0001$ for all). VILI scores decreased in the rTM, rAT, and rTMAT groups compared with those in the HTV group ($P<0.0001$ for all; Fig. 4H).

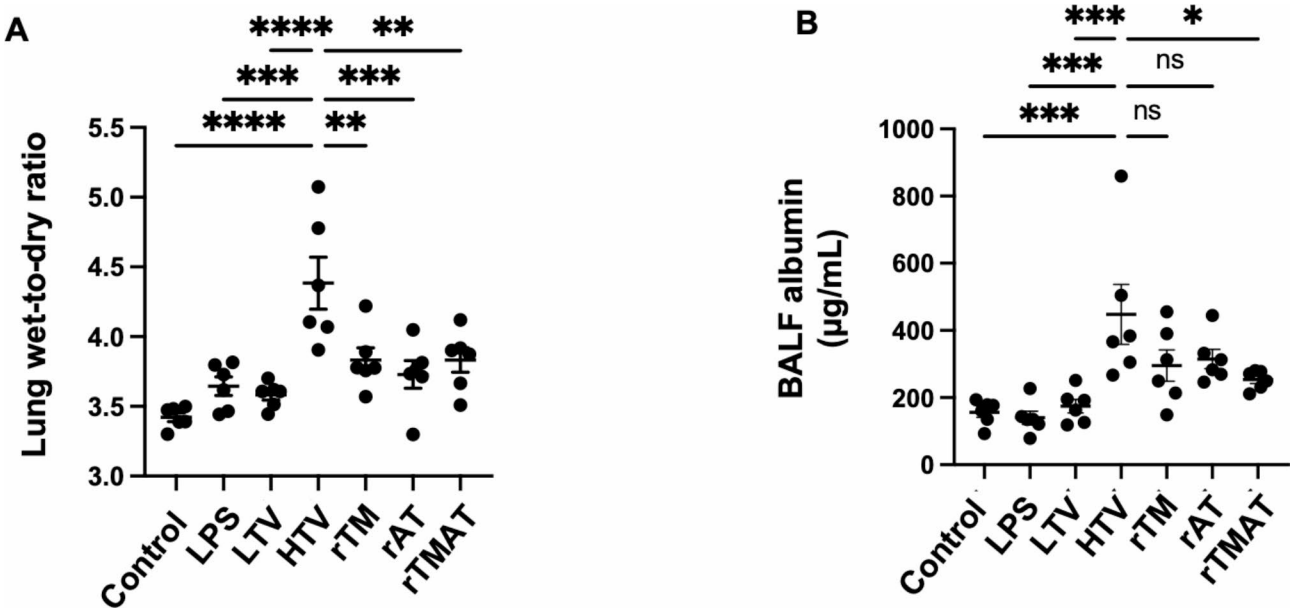

Fig. 3 Pulmonary vascular permeability. **A**) Lung wet-to-dry ratio ($N=6$). Lung wet-to-dry ratio was calculated as (wet weight – dry weight) / (dry weight) of each sample. **B**) BALF albumin levels ($N=6$). ns = not significant. *$P \le 0.05$, **$P \le 0.01$, ***$P \le 0.001$, ****$P \le 0.0001$. BALF = bronchoalveolar lavage fluid

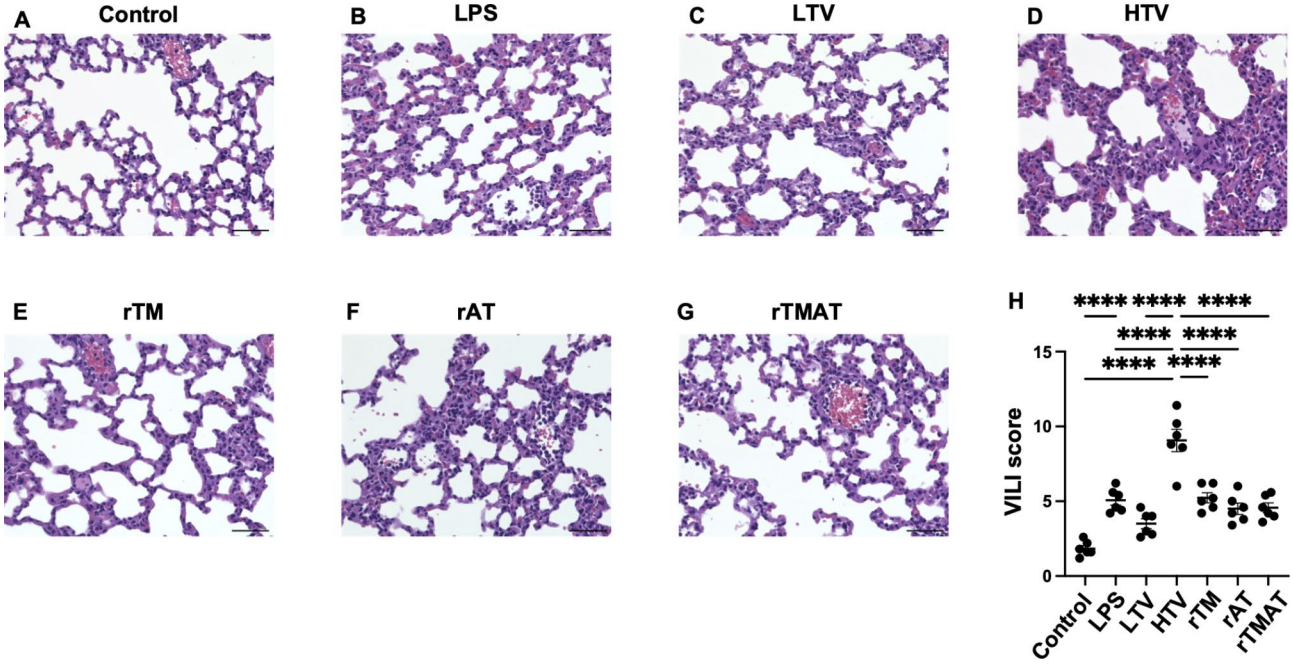

Fig. 4 Lung histology in VILI. **A–G**) Representative images of hematoxylin-eosin staining of the lungs in each group. Alveolar wall thickening, neutrophilic infiltration, and hemorrhage were observed in the LPS group (B) and were more severe in the HTV group (D). These features were reduced in the rTM, rAT, and rTMAT groups (E–G). Scale bar = 50 μm. **H**) Quantitative analysis of lung injury was performed using VILI score ($N=6$). The degree of lung injury was quantitatively assessed by adding up the scores, ranging from 0 (minimal damage) to 12 (maximal damage). *$P \le 0.05$, **$P \le 0.01$, ***$P \le 0.001$, ****$P \le 0.0001$. LPS = lipopolysaccharide; rTM = recombinant thrombomodulin; rAT = recombinant antithrombin; HTV = high tidal volume ventilation; VILI = ventilator-induced lung injury

Effect of rTM and/or rAT on lung mechanics in VILI

Intra- and intergroup comparisons of hourly changes in PIP and DLP were performed. In all groups, PIP was lower at the start of mechanical ventilation than at any other time point. There was no intergroup difference in PIP, except that the HTV group had higher PIP than the rTMAT group at the end of mechanical ventilation ($P=0.034$; Fig. 5A). Intragroup comparison of DLP showed significantly higher DLP at the beginning of

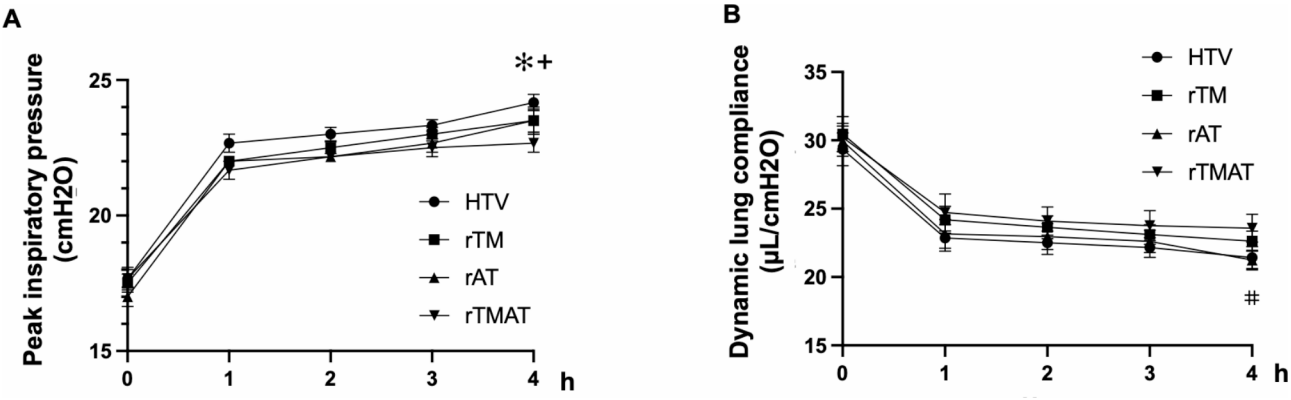

Fig. 5 Changes in peak inspiratory pressure and dynamic lung compliance. (**A**) Hourly changes in PIP from the start of mechanical ventilation to 4 h ($N=6$). PIP at the end of mechanical ventilation was higher in the HTV group than in the rTMAT group ($^{*}P<0.05$). PIP at the beginning of mechanical ventilation was lower than at any other time point in all groups. PIP at 4 h was higher than that at 1 h in the HTV group ($^{+}P<0.01$). (**B**) Hourly changes in DLP from the start of mechanical ventilation to 4 h ($N=6$). There was no difference in DLP between groups at any time point. DLP was higher at the beginning of mechanical ventilation than at any other time point in all groups. DLP at 4 h was lower than that at 1 h in the HTV group ($^{\#}P<0.05$). PIP = peak inspiratory pressure; DLP = dynamic lung compliance; HTV = high tidal volume ventilation

mechanical ventilation in all groups than at any other time point. In the HTV group, DLP at 4 h was lower than that at 1 h ($P=0.012$). There was no significant intergroup difference in DLP at any time point (Fig. 5B).

Effect of rTM and/or rAT on glycocalyx dynamics in VILI

Serum syndecan-1 levels were significantly higher in the LPS group than in the control group ($P<0.0001$) and even higher in the HTV group ($P=0.031$). rTM, rAT, and rTMAT reduced serum syndecan-1 levels ($P<0.0001$ for all; Fig. 6A). *Lycopersicon esculentum* lectin binds to glycocalyx. The low immunofluorescence intensity of the fluorescently labeled tomato lectin indicates a high degree of glycocalyx injury. In the control group, a lectin with high fluorescence intensity was observed throughout the field. In the LPS and HTV groups, lectin fluorescence significantly reduced throughout the field. The fluorescence intensity was recovered in all treatment groups (Fig. 6B). Quantitative evaluation of fluorescence intensity showed that the fluorescence intensity of lectin significantly decreased in the LPS and HTV groups compared with that in the control group ($P<0.0001$ for both), and the decrease in fluorescence intensity was reversed by rTM, rAT, and rTMAT ($P<0.0001$ for all; Fig. 6C). In TEM images, a continuous layer of glycocalyx was observed in the lumen of vessels in the control group, whereas a partial deviation of the glycocalyx layer into the lumen of vessels and thinning of the glycocalyx layer was observed in the LPS group; these were more severe in the HTV group. The damaged glycocalyx aggregates spherically and is released into the vessel lumen. Therapeutics prevented thinning and loss of the glycocalyx layer (Fig. 6D). The occupied area of the glycocalyx in the vascular lumen was significantly reduced in the LPS and HTV groups compared with that in the control group ($P<0.0001$ for both). LTV restored the glycocalyx layer better than spontaneous breathing with LPS ($P<0.0001$). The glycocalyx-occupied area was significantly increased in the rTM, rAT, and rTMAT groups compared with that in the HTV group ($P<0.0001$ for all; Fig. 6E).

Effect of rTM and/or rAT on NET formation in VILI

The ds-DNA is a component of NETs. Leakage of ds-DNA into BALF suggests lung NET formation [5, 25]. BALF ds-DNA levels increased by LPS and further by HTV ($P=0.0027$ and $P=0.007$, respectively). rAT and rTMAT decreased BALF ds-DNA levels ($P=0.0014$ and $P<0.0001$, respectively; Fig. 7A). Colocalization of citrullinated histone H3 and MPO indicated NET formation and was rarely observed in the control, rTM, rAT, and rTMAT groups. Slight colocalization was observed in the LPS and LTV groups, and a significant increase in colocalization was observed in the HTV group (Fig. 7B). The percentage of citrullinated histone H3-positive areas was greater in the HTV group than in the control, LPS, and LTV groups ($P<0.0001$, $P=0.0183$, and $P<0.0001$, respectively). rTM, rAT, and rTMAT administration resulted in a smaller area of citrullinated histone H3 ($P=0.0002$, $P=0.0002$, and $P<0.0001$, respectively; Fig. 7C). The percentage of MPO-positive area was greater in the HTV group than in the control, LPS, and LTV groups ($P<0.0001$, $P=0.0035$, and $P<0.0001$, respectively). MPO-positive areas were smaller in the rTM, rAT, and rTMAT groups than in the HTV group ($P<0.0001$ for all; Fig. 7D).

Discussion

We showed that VILI was induced by LPS and HTV for 4 h, eGCX was injured, and NET formation was significantly increased. We also showed that rTM, rAT, and

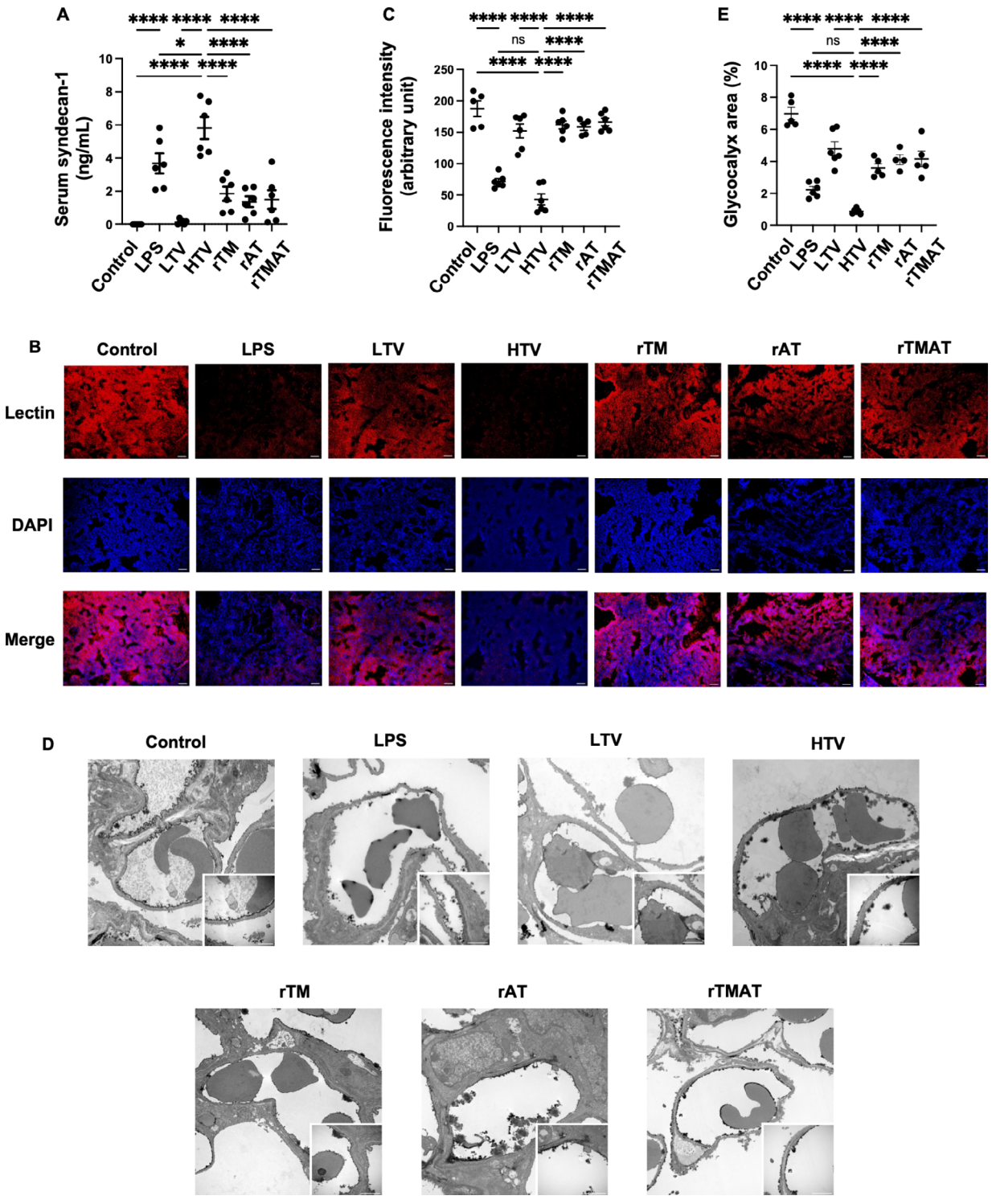

Fig. 6 Degradation of the endothelial glycocalyx. (**A**) Serum syndecan-1 levels ($N=6$). (**B**) Representative images of fluorescent lectin staining of the lung for each group. The lectin-bound glycocalyx is shown in red, and the DNA is shown in blue. Scale bar = 50 μm. (**C**) Lectin fluorescence intensity for each group ($N=5$–6). (**D**) Representative images of the glycocalyx by transmission electron microscopy. A continuous glycocalyx layer was observed in the control group. The glycocalyx was removed from the endothelium, and the glycocalyx layer was thin and disrupted in the LPS and HTV groups. Spherical aggregation of the glycocalyx layer was observed in the HTV group. The deviation and thinning of the glycocalyx decreased in the rTM, rAT, and rTMAT groups. Low and high magnification images for each group. Scale bar = 1 μm. (**E**) The percentage of glycocalyx area in the vascular lumen ($N=4$–6). ns = not significant. $^{*}P \le 0.05$, $^{**}P \le 0.01$, $^{***}P \le 0.001$, $^{****}P \le 0.0001$. HTV = high tidal volume ventilation; LPS = lipopolysaccharide; rTM = recombinant thrombomodulin; rAT = recombinant antithrombin

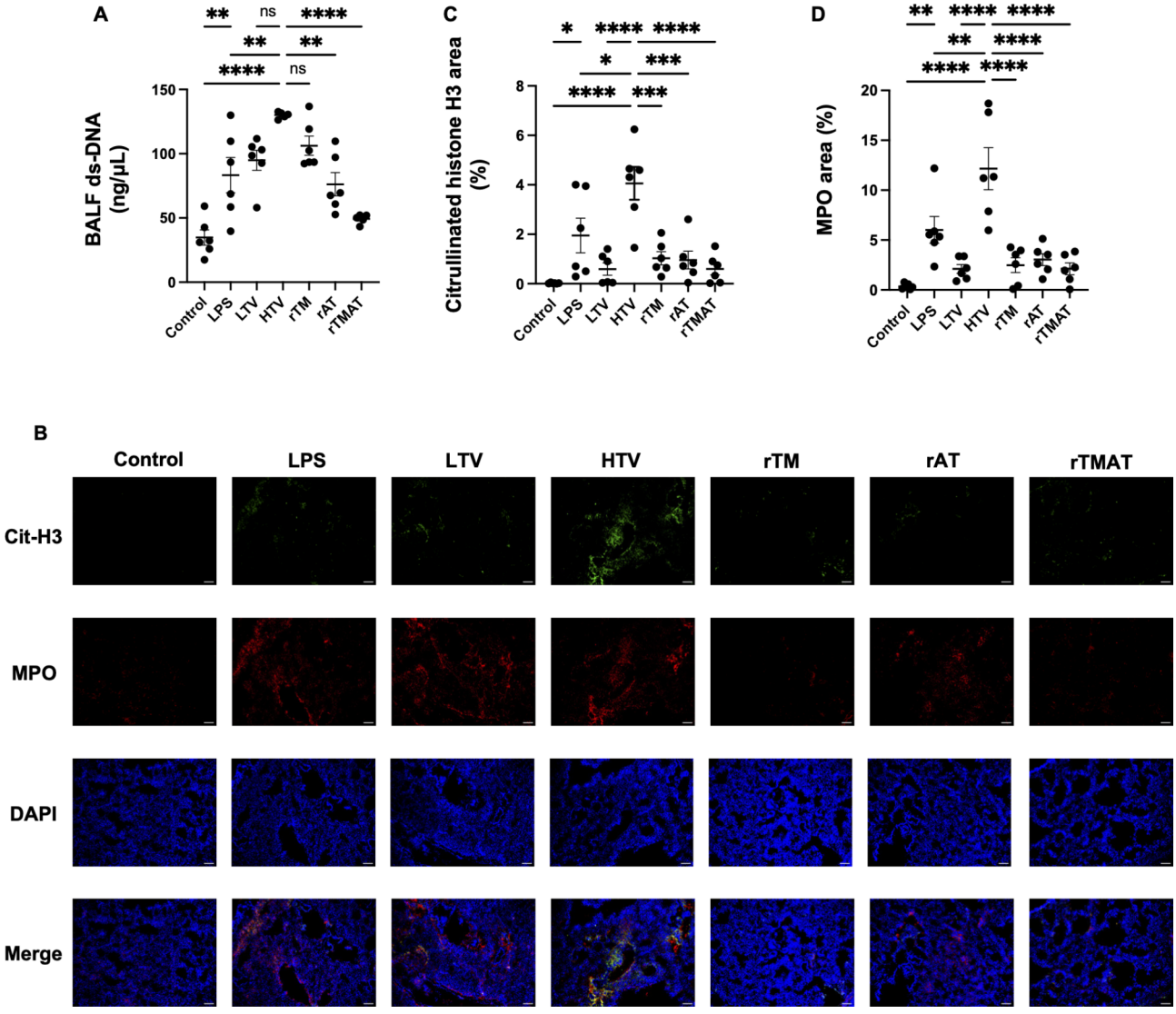

Fig. 7 NET formation in VILI. (**A**) BALF ds-DNA levels ($N = 5–6$). (**B**) Representative immunofluorescence images of NET formation in the lung. Citrullinated histone H3 is shown in green (Cit-H3), MPO in red, and DNA in blue (DAPI). There was extensive colocalization of citrullinated histone H3 and MPO in the HTV group and weak colocalization in the LTV and LPS groups. Colocalization was significantly reduced in the rTM, rAT, and rTMAT groups compared with that in the HTV group. Scale bar = 50 μm. **C**, **D**) The percentage of Cit-H3-positive ($N = 6$) and MPO-positive ($N = 6$) area. ns = not significant; Cit-H3 = citrullinated histone H3. $^{*}P \le 0.05$, $^{**}P \le 0.01$, $^{***}P \le 0.001$, $^{****}P \le 0.0001$. HTV = high tidal volume ventilation; LTV = low tidal volume ventilation; LPS = lipopolysaccharide; rTM = recombinant thrombomodulin; rAT = recombinant antithrombin

rTMAT prevented eGCX injury and NET formation. These results suggest that eGCX injury and NET formation play roles in biotrauma on VILI, and either or both rTM and rAT may serve as potential prophylactic agents for this condition.

In our VILI model, systemic and pulmonary inflammation increased, pulmonary vascular permeability increased, and histological lung injury occurred (Figs. 2, 3 and 4). Previous studies have often included only HTV to induce VILI. This model has the advantage of studying biological responses to invasive mechanical ventilation but may not be suitable for studying NETs because of low pulmonary neutrophil infiltration [5]. Our model is suitable for studying NETs because neutrophil infiltration into the lungs increased (Figs. 2F and 4), and it is similar to actual clinical practice because patients who are mechanically ventilated often have underlying inflammatory diseases.

eGCX thickness is reduced in critically ill patients on mechanical ventilation [26], and VILI increases inflammatory cytokines and oxidative stress [27].

Supraphysiological HTV induces the progression of inflammation from the alveolar epithelium to the endothelium. No study has investigated the relationship between eGCX and VILI. We showed that the degree of eGCX injury was significantly greater in the HTV group

than in the control, LPS, and LTV groups (Fig. 6). This result suggests that LPS-induced inflammation and supraphysiological ventilation synergistically exacerbate eGCX injury. Although there was no significant difference in histological injury between the LPS and LTV groups, the LTV group tended to have less histological lung injury than the LPS group (5.1±0.3 vs. 3.5±0.3, $P=0.12$) (Fig. 4). A significant reduction in eGCX degradation was observed in the LTV group compared to the LPS group (Fig. 6). It is possible that physiological disturbances such as hypoxia, acidosis, or shock were induced by LPS administration, and these physiological disturbances were partially prevented by low tidal volume mechanical ventilation. In the clinical setting, this situation is explained by the fact that lung protective ventilation could prevent physiological disturbances in septic patients with hypoxia or shock.

Although NETs are useful for maintaining localized infections, excessive NETs can lead to endothelial injury and organ damage. NETs can cause eGCX injury and loss of normal endothelial function through the direct effect of MPO or histone-complexed DNA and the indirect effect of increased inflammatory mediators or oxidative stress [28, 29]. Previous reports showed that an increase in NET formation by sterile inflammation, including ischemia-reperfusion injury [11] or chemical burns [25], was associated with disease exacerbation. The results that NETs and lung injury increased in the HTV group suggested that NETs may have contributed to VILI pathogenesis (Figs. 4 and 7).

rTM and rAT significantly reduced eGCX injury, NET formation, and lung injury in VILI (Figs. 4 and 6, and 7). It is reported that rTM reduces organ damage by maintaining the expression of eGCX components and increasing the expression of anti-inflammatory substances. rTM effects on excessive NETs include the inhibition of histone citrullination by binding to the Mac-1 receptor on neutrophils [30], direct neutralization to histones and HMGB-1 [31], and indirect effects by suppressing inflammatory cytokines. These effects reduce organ damage and mortality. Increases in TNF-α and HMGB-1 levels and neutrophil infiltration, which were rTM targets, were observed in our study (Fig. 2). These results suggest that rTM mitigates lung injury by suppressing eGCX injury and NET formation. The effects of rAT on eGCX and NETs were comparable to those of rTM in this study. A previous study reported that rAT attenuated lung injury and reduced eGCX injury by promoting DNA repair [10] and NET formation by suppressing CXCL2 and HMGB-1 expression, inhibiting neutrophil accumulation [12]. From the results of this study and previous reports, rAT could have suppressed eGCX injury and NETs by partially similar and partially different mechanisms by rTM.

The combination of rTM and rAT in our VILI model effectively attenuated eGCX injury, NET formation and lung injury; however, there was negligible difference between combination therapy and monotherapy. No synergistic effects of monotherapy were observed in combination therapy. Few studies have investigated the combination therapy of rTM and rAT in vivo. A report claimed that leukocyte adhesion to the endothelium and HMGB-1 levels was significantly reduced by combination therapy, whereas no difference in the markers of organ damage was observed between monotherapy and combination therapy [32]. However, mortality was reduced by combination therapy [33], or organ damage, histone H3 levels, and ds-DNA levels were reduced by combination therapy [34]. In clinical trials, some reports showed no difference in the treatment of septic disseminated intravascular coagulation with the combination compared with antithrombin alone [35], whereas others reported that the combination improved patient prognosis [36]. In the present study, combination therapy did not differ from monotherapy with respect to eGCX or lung injury. Only BALF ds-DNA levels were lower in the rTMAT group than in the rTM group (Fig. 7A); however, the area of NETs was the same (Fig. 7B-D). The efficacy of monotherapy or combination therapy may vary depending on disease severity, drug dosage, and timing of drug injection. These factors may explain the lack of significant differences observed in this study.

This study has several limitations. First, using a supraphysiological tidal volume (20 mL/kg) may not be directly applicable to critically ill patients in clinical practice. There is a large heterogeneity of high tidal volume in the VILI model, ranging from 12 to 47 mL/kg [37]. However, our model induced inflammatory responses and lung injuries with a tidal volume of 20 mL/kg, indicating certain quantifiable characteristics. Second, only male mice were used in this study. Although the effect of sex hormones on inflammation may have influenced the results, it has been reported that there was little sex-specific difference in the susceptibility to VILI [38]. Our model of VILI in male mice is considered appropriate for testing the hypothesis of this study. Third, we did not assess parameters such as pH, partial pressure of arterial oxygen, or lactate levels, which could impact the results. Fourth, the efficacies of rTM, rAT, and rTMAT were primarily studied in models of sepsis [32–34], ARDS [9, 10], or ischemia-reperfusion injury [11, 31], not in models of VILI. Therefore, it was difficult to directly apply these results to the VILI model. Conversely, sepsis and VILI share pathophysiological similarities in terms of organ dysfunction syndrome and inflammation-induced vascular endothelial injury. In our VILI model, endothelial injury (eGCX injury and NET formation) occurred. Given the effect of rTM, rAT, and rTMAT on

vascular endothelial injury based on previous reports [9, 10, 32], they may also be effective in treating VILI. Our results showed that rTM and/or rAT effectively reduced biotrauma. Finally, while this study did not establish a direct relationship between eGCX and NET formation, increased MPO and extracellular DNA, as well as their reduction with therapeutics, indirectly suggests that NETs induced by VILI interfere with eGCX. Future research should investigate eGCX injury and NET formation with varying tidal volumes and the therapeutic effects of rTM or rAT to address these limitations. Additionally, a comprehensive evaluation of lung function in VILI is warranted.

Conclusions

VILI was induced by HTV and LPS. eGCX was degraded, and NET formation increased in VILI. rTM and rAT partially prevented systemic and pulmonary inflammation, lung injury, eGCX degradation, and NET formation in VILI. However, neither affected dynamic lung compliance. There was no synergistic effect when using the rTM and rAT combination compared to when rTM or rAT was used alone.

Abbreviations

ARDS	Acute respiratory distress syndrome
BALF	Bronchoalveolar lavage fluid
DLP	Dynamic lung compliance
ds-DNA	Double-stranded DNA
eGCX	Endothelial glycocalyx
ELISA	Enzyme-linked immunosorbent assay
LPS	Lipopolysaccharide
MPO	Myeloperoxidase
NETs	Neutrophil extracellular traps
PBS	Phosphate-buffered saline
PIP	Peak inspiratory pressure
rAT	Recombinant antithrombin
rTM	Recombinant thrombomodulin
TEM	Transmission electron microscopy
VILI	Ventilator-induced lung injury

Acknowledgements

The authors thank Hirohisa Okushima and Yuko Hayakawa for assistance with transmission electron microscopy. The authors also thank Yasuaki Sawashita and Yuri Horiguchi for their technical assistance. Asahi Kasei Pharma (Tokyo, Japan) provided recombinant thrombomodulin and Kyowa Kirin Co., Ltd (Tokyo, Japan) provided recombinant antithrombin but did not contribute to the study design, data collection, data analysis or preparation of the manuscript.

Author contributions

KK and SK designed the study. KK performed the animal studies. SK helped with the animal studies. KK, SK, and MY analyzed and interpreted the data. KK was a major contributor in writing the manuscript. SK and MY reviewed and edited the manuscript. All authors read and approved the final manuscript.

Funding

This study was supported by JSPS KAKENHI (Grant number 22K09123) and by the Osaka Medical Research Foundation for Intractable Diseases (Grant number 28-2-9).

Data availability

No datasets were generated or analysed during the current study.

Declarations

Ethics approval and consent to participate

This study was approved by the Institutional Animal Care and Use Committee of Sapporo Medical University (approval number 20–097) and adhered to the Guide for the Care and Use of Laboratory Animals. This article was conducted in compliance with the ARRIVE guidelines.

Consent for publication

Not applicable.

Competing interests

The authors declare no competing interests.

Author details

[1]Department of Anesthesiology, School of Medicine, Sapporo Medical University, S-1, W-16 Chuo-ku, Sapporo 060-8543, Hokkaido, Japan
[2]Department of Intensive Care Medicine, School of Medicine, Sapporo Medical University, S-1, W-16 Chuo-ku, Sapporo 060-8543, Hokkaido, Japan

Received: 6 June 2024 / Accepted: 20 August 2024
Published online: 03 September 2024

References

1. Slutsky AS, Ranieri VM. Ventilator-induced lung injury. N Engl J Med. 2013;369:2126–36.
2. Ricard JD, Dreyfuss D, Saumon G. Ventilator-induced lung injury. Eur Respir J Suppl. 2003;42:s2–9.
3. Curley GF, Laffey JG, Zhang H, Slutsky AS. Biotrauma and ventilator-induced lung injury: clinical implications. Chest. 2016;150:1109–17.
4. Moore KH, Murphy HA, George EM. The glycocalyx: a central regulator of vascular function. Am J Physiol Regul Integr Comp Physiol. 2021;320:R508–18.
5. Yildiz C, Palaniyar N, Otulakowski G, Khan MA, Post M, Kuebler WM, et al. Mechanical ventilation induces neutrophil extracellular trap formation. Anesthesiology. 2015;122:864–75.
6. Manchanda K, Kolarova H, Kerkenpaß C, Mollenhauer M, Vitecek J, Rudolph V, et al. MPO (myeloperoxidase) reduces endothelial glycocalyx thickness dependent on its cationic charge. Arterioscler Thromb Vasc Biol. 2018;38:1859–67.
7. Russell RT, Christiaans SC, Nice TR, Banks M, Mortellaro VE, Morgan C, et al. Histone-complexed DNA fragments levels are associated with coagulopathy, endothelial cell damage, and increased mortality after severe pediatric trauma. Shock. 2018;49:44–52.
8. Schmidt EP, Yang Y, Janssen WJ, Gandjeva A, Perez MJ, Barthel L, et al. The pulmonary endothelial glycocalyx regulates neutrophil adhesion and lung injury during experimental sepsis. Nat Med. 2012;18:1217–23.
9. Suzuki K, Okada H, Takemura G, Takada C, Tomita H, Yano H, et al. Recombinant thrombomodulin protects against LPS-induced acute respiratory distress syndrome via preservation of pulmonary endothelial glycocalyx. Br J Pharmacol. 2020;177:4021–33.
10. Okamoto H, Muraki I, Okada H, Tomita H, Suzuki K, Takada C, et al. Recombinant antithrombin attenuates acute respiratory distress syndrome in experimental endotoxemia. Am J Pathol. 2021;191:1526–36.
11. Hayase N, Doi K, Hiruma T, Matsuura R, Hamasaki Y, Noiri E, et al. Recombinant thrombomodulin on neutrophil extracellular traps in murine intestinal ischemia-reperfusion. Anesthesiology. 2019;131:866–82.
12. Ishikawa M, Yamashita H, Oka N, Ueda T, Kohama K, Nakao A, et al. Antithrombin III improved neutrophil extracellular traps in lung after the onset of endotoxemia. J Surg Res. 2017;208:140–50.
13. Shrestha B, Ito T, Kakuuchi M, Totoki T, Nagasato T, Yamamoto M, et al. Recombinant thrombomodulin suppresses histone-induced neutrophil extracellular trap formation. Front Immunol. 2019;10:2535.
14. Watanabe-Kusunoki K, Nakazawa D, Ishizu A, Atsumi T. Thrombomodulin as a physiological modulator of intravascular injury. Front Immunol. 2020;11:575890.
15. Pal N, Kertai MD, Lakshminarasimhachar A, Avidan MS. Pharmacology and clinical applications of human recombinant antithrombin. Expert Opin Biol Ther. 2010;10:1155–68.

16. Rezaie AR, Giri H, Antithrombin. An anticoagulant, anti-inflammatory and antibacterial serpin. J Thromb Haemost. 2020;18:528–33.
17. Kawai S, Takagi Y, Kaneko S, Kurosawa T. Effect of three types of mixed anesthetic agents alternate to ketamine in mice. Exp Anim. 2011;60:481–7.
18. Chen R, Zeng L, Zhu S, Liu J, Zeh HJ, Kroemer G, et al. cAMP metabolism controls caspase-11 inflammasome activation and pyroptosis in sepsis. Sci Adv. 2019;5:eaav5562.
19. Matute-Bello G, Downey G, Moore BB, Groshong SD, Matthay MA, Slutsky AS, et al. An official American Thoracic Society workshop report: features and measurements of experimental acute lung injury in animals. Am J Respir Cell Mol Biol. 2011;44:725–38.
20. Sun L, Hult EM, Cornell TT, Kim KK, Shanley TP, Wilke CA, et al. Loss of myeloid-specific protein phosphatase 2A enhances lung injury and fibrosis and results in IL-10-dependent sensitization of epithelial cell apoptosis. Am J Physiol Lung Cell Mol Physiol. 2019;316:L1035–48.
21. Faller S, Ryter SW, Choi AMK, Loop T, Schmidt R, Hoetzel A. Inhaled hydrogen sulfide protects against ventilator-induced lung injury. Anesthesiology. 2010;113:104–15.
22. Okada H, Takemura G, Suzuki K, Oda K, Takada C, Hotta Y, et al. Three-dimensional ultrastructure of capillary endothelial glycocalyx under normal and experimental endotoxemic conditions. Crit Care. 2017;21:261.
23. Sawashita Y, Kazuma S, Tokinaga Y, Kikuchi K, Hirata N, Masuda Y, et al. Albumin protects the ultrastructure of the endothelial glycocalyx of coronary arteries in myocardial ischemia-reperfusion injury in vivo. Biochem Biophys Res Commun. 2023;666:29–35.
24. Inagawa R, Okada H, Takemura G, Suzuki K, Takada C, Yano H, et al. Ultrastructural alteration of pulmonary capillary endothelial glycocalyx during endotoxemia. Chest. 2018;154:317–25.
25. Surolia R, Li FJ, Wang Z, Kashyap M, Srivastava RK, Traylor AM, et al. NETosis in the pathogenesis of acute lung injury following cutaneous chemical burns. JCI Insight. 2021;6:e147564.
26. Rovas A, Osiaevi I, Buscher K, Sackarnd J, Tepasse P-R, Fobker M, et al. Microvascular dysfunction in COVID-19: the MYSTIC study. Angiogenesis. 2021;24:145–57.
27. Wagner J, Strosing KM, Spassov SG, Lin Z, Engelstaedter H, Tacke S, et al. Sevoflurane posttreatment prevents oxidative and inflammatory injury in ventilator-induced lung injury. PLoS ONE. 2018;13:e0192896.
28. Hirota T, Levy JH, Iba T. The influence of hyperglycemia on neutrophil extracellular trap formation and endothelial glycocalyx damage in a mouse model of type 2 diabetes. Microcirculation. 2020;27:e12617.
29. Zhang H, Wang Y, Qu M, Li W, Wu D. Neutrophil, neutrophil extracellular traps and endothelial cell dysfunction in sepsis. Clin Transl Med. 2023;13:e1170.
30. Watanabe-Kusunoki K, Nakazawa D, Kusunoki Y, Kudo T, Hattanda F, Nishio S, et al. Recombinant thrombomodulin ameliorates autoimmune vasculitis via immune response regulation and tissue injury protection. J Autoimmun. 2020;108:102390.
31. Hayase N, Doi K, Hiruma T, Matsuura R, Hamasaki Y, Noiri E, et al. Recombinant thrombomodulin prevents acute lung injury induced by renal ischemia-reperfusion injury. Sci Rep. 2020;10:289.
32. Iba T, Miki T, Hashiguchi N, Yamada A, Nagaoka I. Combination of antithrombin and recombinant thrombomodulin attenuates leukocyte-endothelial interaction and suppresses the increase of intrinsic damage-associated molecular patterns in endotoxemic rats. J Surg Res. 2014;187:581–6.
33. Iba T, Nakarai E, Takayama T, Nakajima K, Sasaoka T, Ohno Y. Combination effect of antithrombin and recombinant human soluble thrombomodulin in a lipopolysaccharide induced rat sepsis model. Crit Care. 2009;13:R203.
34. Iba T, Miki T, Hashiguchi N, Tabe Y, Nagaoka I. Combination of antithrombin and recombinant thrombomodulin modulates neutrophil cell-death and decreases circulating DAMPs levels in endotoxemic rats. Thromb Res. 2014;134:169–73.
35. Umegaki T, Kunisawa S, Nishimoto K, Kamibayashi T, Imanaka Y. Effectiveness of combined antithrombin and thrombomodulin therapy on in-hospital mortality in mechanically ventilated septic patients with disseminated intravascular coagulation. Sci Rep. 2020;10:4874.
36. Iba T, Hagiwara A, Saitoh D, Anan H, Ueki Y, Sato K, et al. Effects of combination therapy using antithrombin and thrombomodulin for sepsis-associated disseminated intravascular coagulation. Ann Intensive Care. 2017;7:110.
37. Joelsson JP, Ingthorsson S, Kricker J, Gudjonsson T, Karason S. Ventilator-induced lung-injury in mouse models: is there a trap? Lab Anim Res. 2021;37:30.
38. López-Alonso I, Amado-Rodriguez L, López-Martínez C, Huidobro C, Albaiceta GM. Sex susceptibility to ventilator-induced lung injury. Intensive Care Med Exp. 2019;7:7.

Publisher's note